HYPERSPECTRAL CORE LOGGING MINERAL CHARACTERISATION - NORTHPARKES E48 PORPHYRY Cu-Au DEPOSIT, NSW

Melissa Quigley[1], Jonathon Hoye[2] and Corey Jago[3]

[1.] *Spectral Geoscience Pty Ltd, Sydney, NSW, Australia*
[2.] *CMOC Northparkes Mines, Parkes, NSW, Australia*
[3.] *PO Box 1328, Oxley, QLD, Australia*

Key Words: Northparkes, E48, porphyry, copper, gold, alteration, hyperspectral infrared core logging, Goonumbla Volcanic Complex, Macquarie Arc, HyLogger, mineral characterisation.

ABSTRACT

The Endeavour 48 (E48) Cu-Au porphyry deposit at Northparkes is located in the Junee – Narromine Volcanic Belt of the Ordovician Macquarie Arc, in central New South Wales. Distal to proximal hydrothermal alteration associated with E48 was mineralogically characterised and spatially delineated in a hyperspectral core logging study. Continuous, down-hole mineralogical classification of the extensively altered Goonumbla Volcanics, in and around the E48 deposit was achieved using HyLogger VNIR – SWIR + TIR hyperspectral core logging data and *The Spectral Geologist* (TSG) software, on a ~1000 m deep representative diamond drill hole (E48D134).

Dominant minerals identified from the E48D134 HyLogger spectra include plagioclase, quartz and white mica. Subordinate chlorite and epidote are present in moderate abundance. Kaolinite, montmorillonite, goethite, hematite, goethite, gypsum, carbonate, microcline, biotite and phlogopite occur in minor abundance. Trace amounts of dickite and hornblende were also identified.

The distribution and abundance of key indicator minerals identified from the infrared data spatially delineated four distinct porphyry-related hydrothermal alteration zones extending from the distal parts of the system to the central ore zone including; distal propylitic, outer potassic, inner potassic and a central phyllic zone.

Previously unrecognised inter-zonal mineralogical variations were identified by the isomorphous substitution of Al in the white micas and Fe-Mg in chlorites. This provided insight to the temperature and pH physicochemical conditions associated with the formation of the E48 porphyry deposit.

The study demonstrates how the spectral fingerprints of minerals can be used to spatially define and characterise the hydrothermal alteration footprints associated with Cu-Au porphyry deposits.

INTRODUCTION

Northparkes Mines is a copper-gold mining operation located at Goonumbla, approximately 27 kilometres north- northwest of the town of Parkes in Central West New South Wales, Australia. Porphyry-copper type mineralisation at Northparkes was discovered in 1976 by Geopeko Ltd. (Lye, 2010) , with open cut operations on the E22 and E27 deposits commencing in 1993 (Lye, 2006) . Subsequent mining operations have focussed on underground mass mining from the E26 and E48 deposits, primarily by the block caving method, with the E26L1 being the first operation of this type in Australia, commencing operations in 1996.

To date, mining has produced 860,000 tonnes of copper and 1,200,000 ounces of gold from four main deposits (E22, E26, E27, and E48), with current combined JORC Ore Reserves and Resources of 602.69 million tonnes at 0.56% Cu and 0.19g/t Au (CMOC, 2017).

Due to the paucity of outcrop and significant regolith cover in the Northparkes Mines (NPM) tenement package, an emphasis is placed on maximising the information obtained from drill core. Hyperspectral core logging is a tool to assist geologists meet that objective by extracting continuous, down-hole mineralogical information to characterise the regolith, alteration and host rock associated with ore deposits (Huntington et al., 2006; Huntington J. F. and P., 2008; Quigley, 2009).

NPM have acquired HyLogger-3 hyperspectral infrared core logging data from eight diamond drill holes from the E26 and E48 deposits totalling 5056.9m. The data will be analysed with the aim of determining the spectral characteristics of the main alteration zones from the distal parts of the porphyry mineral systems to the central ore zones. Developing spectro-mineralogical proximity indicators can provide insight to the reconstruction of the physico-chemical (e.g. pH and temperature) environment of ore formation, further the 3D understanding of a deposit's mineral system and provide a framework to guide regional exploration.

The hyperspectral core analysis study forms part of the evolving Northparkes exploration program. This paper reports on the hyperspectral mineralogical characterisation and spatial distribution of the constituent mineralogy for diamond drill hole E48D134, a representative drill hole from the E48 alkalic Cu-Au porphyry deposit.

GEOLOGICAL SETTING

The Northparkes Cu-Au porphyry deposits are hosted within the Ordovician Wombin and Goonumbla Volcanics, collectively termed the Goonumbla Volcanic Complex (GVC) (Simpson, 2000) that form part of the north – south trending Junee – Narromine Volcanic Belt of the Lachlan Orogen in central NSW (Glen et al., 2007; Glen et al., 1998) . The GVC consist of a broadly folded sequence of andesitic to trachytic volcanics and volcaniclastic sediments.

The Endeavour deposits are variants of silica saturated, alkalic, porphyry Cu-Au systems, with mineralisation centred on discrete polyphasal monzonite porphyries with relatively limited lateral extent (5 - 100 m), but displaying significant vertical continuity (over 1 km). The quartz monzonite porphyry (QMP) pipes and dykes have intruded both the GVC and pre-mineral equigranular monzonitic stocks that predominate at depth (Lickfold et al., 2003).

Copper sulphide mineralisation occurs predominantly within stockwork quartz±anhydrite veins and as fine disseminations in both the country rock and porphyries, with lesser sheeted quartz vein-hosted and fracture coat sulphides. Highest hypogene copper grades tend to be associated with areas of increased quartz vein density in the country rock immediately surrounding the early syn-mineral porphyries.

Sulphide species in the systems are zoned from bornite-dominant cores, centred on the quartz monzonite porphyries, outwards through a chalcopyrite-dominant zone, with a poorly defined distal pyrite halo tending to be slightly separate from the inner copper bearing zones. Gold within the porphyry systems at Northparkes tends to occur as fine (<10μm) free gold or electrum inclusions within bornite in the core of each system (House, 1994).

Hydrothermal alteration assemblages tend to vary between deposits within the district, generally being zoned around the quartz monzonite porphyries, with a central K-feldspar-hematite±white mica alteration assemblage surrounded by biotite magnetite (metasomatic) alteration zones, ranging out to poorly defined actinolite subzones at the E22 and E27 deposits, epidote-chlorite-hematite

assemblages (propylitic), and distal chlorite-carbonate±zeolite facies. The scale of each assemblage is a function of host rock composition and hydrothermal fluid flux, with the inner K-feldspar alteration zone extending up to 100-200 metres outboard from the porphyry at the E26 and GRP314 deposits, in contrast to the E22, E27, and E48 deposits where K-feldspar alteration is generally more restricted. Biotite-magnetite alteration forms a halo up to 200m outboard from the mineralising porphyries, tending to be more strongly developed at the E22, and E27, resulting in annular magnetic high features in geophysical datasets. The E48 deposit differs from other systems in having a well-developed hematite-white mica±carbonate alteration assemblage largely overprinting earlier potassic alteration around the core of mineralisation. Assemblages of pervasive white mica-albite±quartz occur at depth in most systems, related to high temperature magmatic-hydrothermal fluids (Lickfold et al., 2007; Wolfe, 1994).

Late syn-mineral to post mineralisation deformation has resulted in the development of east-dipping low-angle faulting with an inferred thrust sense, which truncates mineralisation at E48 and extends from east of the E26 deposit to north of the former E27 pit. Post-mineral deformation is generally limited, with gentle tilting of the mine block resulting in orebodies having a steep north-northeasterly plunge (~83°).

The focus of this study is on diamond drill hole E48D134, a representative drill hole from the E48 deposit. The top of the E48 deposit was dislocated by the shallow east dipping Altona Fault, obscuring E48 from surface. E48D134 is drilled east to west and extends from the base of the Altona Fault on the eastern margin of the deposit, to an inclined depth of 1014.15 m intersecting mineralised quartz monzonite porphyry intrusions towards the end of the hole.

METHODOLOGY

Hyperspectral Core Logging Data Collection

Diamond drill hole E48D134 was scanned with a HyLogger-3 at the Geological Survey of New South Wales' WB Clarke Geoscience Centre at Londonderry in early 2017.

The HyLogger-3 automated the rapid and systematic collection of infrared reflectance measurements from the visible – near infrared (VNIR; 380 – 1000 nm), shortwave infrared (SWIR; 1000 – 2500 nm) and thermal infrared (TIR; 6000 – 14500 nm) regions across the electromagnetic spectrum. Colour imagery across the full width of the drill core was synchronously acquired with the spectra. A total of 125,942 depth registered VNIR – SWIR + TIR spectra were collected from 894.15 m of E48D134 diamond drill core (120 – 1014.15 m; missing core 1000.1 – 1013.9m) in 189 trays.

Hardware

HyLogging is a non-contact, non-destructive hyperspectral core logging technique for identifying mineralogical information in drill core or chips. The CSIRO- developed HyLogger system (Schodlok et al., 2016) scans full and split drill core and chips in their original trays. Sample preparation generally entails ensuring the core is dry and clean from mud and drillers grease. Scan rates vary according to operational constraints; a five section core tray (5 m) can be scanned in ~5 minutes.

The HyLogger-3 performs a continuous scan capturing calibrated infrared reflectance from a ~10 mm wide field-of-view at ~10 mm spacing along the centre of the core. Each core tray section is sequentially scanned as the core tray is traversed on a robotically controlled X – Y table. The instrument suite mounted ~300 mm above the table consists of three spectrometers, a linescan camera and laser (height measuring) profilometer. A customised halogen lighting configuration

illuminates the core. Linescan imagery was captured across the full width of the core and automatically configured into labelled core tray images.

Each wavelength channel of the HyLogging spectrometers recorded the intensity of reflectance from the surface of the core. A plot of the wavelengths (X-axis) versus the reflectance intensity (Y-axis) produced a spectrum for each sample that serves as a spectral fingerprint of the sample's mineralogy. Infrared spectral features observed in a spectrum are due to the bending and stretching of molecular bonds in a minerals lattice and represent overtones and combination tones of fundamental electronic and vibration processes occurring at longer wavelengths (Clark, 1999; Hunt, 1977; Hunt and Salisbury, 1970). Recognition of the diagnostic reflectance features at specific wavelengths enables the identification of the sample's mineralogy and associated parameters (e.g. relative abundance, compositional substitution and in some minerals, their crystallinity).

Spectrally Identifiable Minerals

The three wavelength regions covered by the HyLogger-3 are complimentary in terms of the minerals able to be detected in each infrared region. For example, the VNIR is best suited to the detection of iron oxides and oxyhydroxides (e.g. hematite and goethite); the SWIR for hydroxyl-bearing silicates (e.g. smectites, white micas, kaolins, chlorite, sulphates, epidote, talc, biotite and amphibole) and carbonate; and the TIR for anhydrous framework silicates (e.g. quartz, feldspar, zeolites, garnet, pyroxene and olivine) as well as carbonates, sulphates and phosphates. Note some minerals display diagnostic spectral features in more than one wavelength region.

Software and Processing

Processing, analysis, interactive visualisation and interpretation of the HyLogging data were carried out in *The Spectral Geologist* [TM] (TSG) software package (version 8.0.2.6) (www.thespectralgeologist.com) developed by the CSIRO (Berman et al., 1999; Berman et al., 2017). Methods utilised for extracting the mineral information included: (i) project specific custom-built scalars targeting single or multiple diagnostic absorption features via polynomial fitting within nominated band (wavelength) intervals and, (ii) mineral class and species extraction routines based on *The Spectral Assistant* (TSA)[TM] algorithm. Geochemistry, magnetic susceptibility and lithology logs were imported into TSG for integration with the spectro-mineralogical results to determine trends, anomalies and relationships between the datasets.

A focus was placed on extracting two of the most informative spectral parameters exhibited in hyperspectral core logging data; 1) the depth of a minerals' diagnostic absorption features, used as a metric/index to convey relative abundance or intensity information, and 2) the wavelength minima of the diagnostic absorption feature, responsive to the chemical bonds in the mineral lattice, providing an indirect measure of composition.

RESULTS and DISCUSSION

The dominant minerals identified from the E48D134 HyLogger spectra include plagioclase, quartz and white mica. Subordinate chlorite and epidote are present in moderate abundance. Kaolinite (poorly crystalline and well crystalline), montmorillonite, goethite, hematite, gypsum, carbonate, microcline, biotite and phlogopite occur in minor abundance. Trace amounts of dickite and hornblende were also identified. Table 1 reports the wavelength regions the minerals were identified in and their relative abundance. The 'spectral signature' or 'spectral fingerprint' of the minor-high abundance minerals are represented in the VNIR – SWIR + TIR spectra in Figure 1.

Table 1.   *Relative abundance of minerals identified in the E48 HyLogger VNIR – SWIR+TIR reflectance data.*

Relative Abundance	VNIR	SWIR	TIR
High		White mica	Plagioclase and quartz.
Moderate		Chlorite, epidote.	
Minor	FeOx (goethite, hematite).	Kaolinite, montmorillonite, gypsum, carbonate, biotite and phlogopite.	K-feldspar (microcline) and carbonate.
Trace		Dickite and hornblende.	
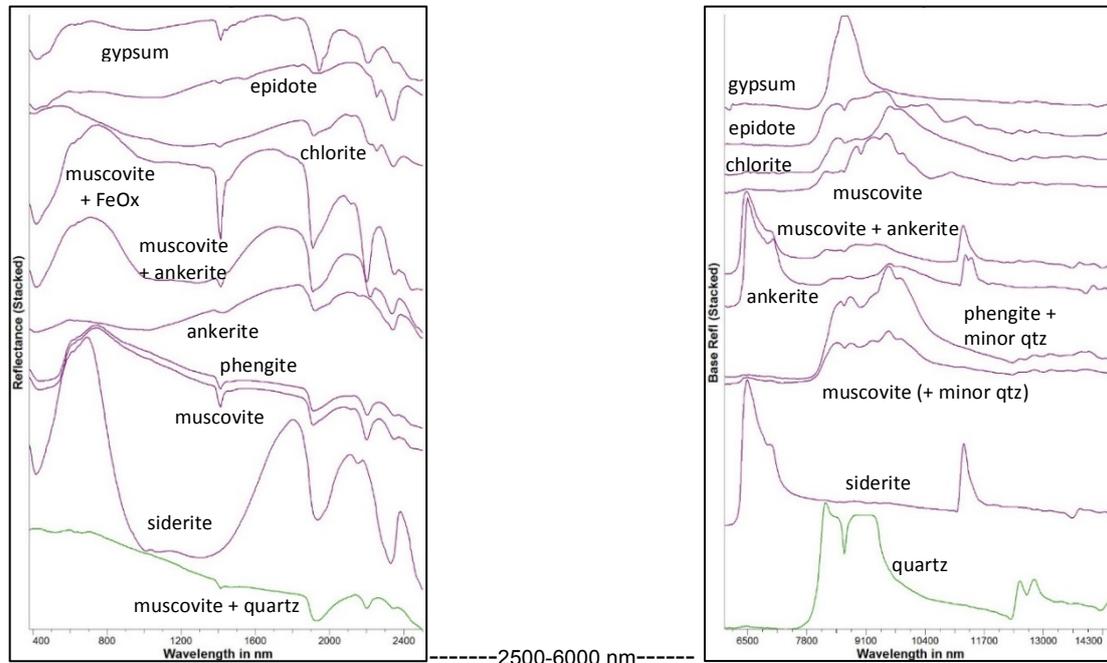
Figure 1.   *VNIR – SWIR + TIR spectra of minerals identified in E48D134's HyLogger-3 spectra.*

The distribution and abundance of key indicator minerals identified from the E48D134 HyLogger data enabled the down-hole logging and spatial delineation of an alteration footprint consisting of four distinct porphyry-related hydrothermal alteration zones;

    1) Distal propylitic zone,
    2) Outer potassic (metasomatic) zone,
    3) Inner potassic/sodic zone and
    4) Deep phyllic zone.

Distal Propylitic Alteration Zone

The propylitic zone in drill hole E48D134 is distal to mineralisation and is delineated as occurring from the base of the Altona Fault at a depth of ~120m to a depth of ~600 m. The propylitic zone is hyperspectrally characterised by the spatial distribution of;

- Extensive, weak-moderately developed chlorite.
- Subordinate, intense epidote.
- Extensive and abundant plagioclase (labradorite, albite, oligoclase).
- Minor quartz, white mica, hematite, goethite, gypsum and ankerite.

Changes within the propylitic zone are evident based mainly on the distribution of epidote (Figure 2a) and chlorite (Figure 2b). Epidote and chlorite share common wavelength features at ~2250 nm and ~2340 nm. In E48D134, the epidote-bearing samples display significantly deeper absorption feature depths compared to those of chlorite-bearing samples. A scalar based on the depth of the 2340 nm absorption feature with a minimum cut-off applied to limit mixed chlorite bearing samples with shallower depths, was used to distinguish the epidote-bearing samples from the chlorite-bearing samples (Figure 2b epidote=yellow – green; chlorite=blues).

Epidote is typically distinguished from chlorite by its diagnostic minor absorption features at 1550 nm and 1830 nm, however one or both of these epidote absorption features can be diluted or completely lost when epidote occurs in mineral mixtures, commonly with chlorite.

The relatively shallow chlorite absorption features displayed at ~2250 nm in this zone infer chlorite alteration is weakly to moderately developed. Chlorite in this zone represents a retrogression of early metasomatic biotite+magnetite alteration prior to overprinting by epidote+hematite. Chlorite distribution extends to ~838 m however the interval from 600 – 828 m is interpreted as a local overprint on earlier outer potassic alteration and as such is discussed in the relevant section below.

Epidote (Figure 2a) alteration occurs as patchy pervasive domains in volcaniclastic units, with selective replacement of phenocrysts and feldspar crystal fragments in coherent volcanics and coarser clastic units.

To improve the clarity in the spread of the chlorite composition-related wavelengths, a moving average smoothing window was applied to a scalar tracking the ~2250 nm Mg/Fe compositional substitution of Fe^{2+} and Mg^{2+} in the octahedral cation sites of the chlorites. The chlorite bearing samples in the propylitic zone (120 – 600 m) transgress the volcanic sandstone (VSS) and volcanic breccia (VBR) lithologies and extend into the latite (LTE) (Figure 3d), indicating alteration is independent of lithological control. The bulk of the chlorite composition is interpreted as intermediate Fe – Mg chlorite in this zone based on the Mg/Fe – OH related wavelengths ranging from ~2250 – 2253 nm.

The relatively homogenous wavelength zone from 313 – 413.45 m (Figure 3b) is governed by the strongly-developed, compositionally stable epidote exerting a greater influence on the spectra than the proportionally lower chlorite.

Narrow (0.5 – 1 m) localised zones of overprinting diffuse white mica (sericitic) alteration are evident as spikes in the white mica crystallinity scatter plot (Figure 3b), occurring from 458.63 m – 593.46 m. The elevated white mica crystallinity values are interpreted as discrete hydrothermal fluid pathways, developed as a response to the ascent of early vapour-phase magmatic fluids derived from the QMP complexes at depth. These zones correlate well with sub-metre scale intervals of grey 'silica-sericite' alteration, which elsewhere at Northparkes are crosscut by main-stage mineralising quartz sulphide vein arrays, implying an early timing.

The same interval also contains intermittent, sporadic occurrences of weak chlorite (+/-partially retrogressed biotite-phlogopite) bearing samples displaying lower wavelengths at ~2246 nm indicating an increase in Mg content (Figure3d). This is observed to represent the start of the transition from the propylitic zone to the outer potassic alteration zone, and may prove to be an important spectro-mineralogical index or exploration vector/indicator for identifying proximity to potassic alteration, higher temperature alteration or 'near miss' scenarios in drilling.

Plagioclase is a major constituent of the propylitic zone occurring throughout the zone. The plagioclase species identified in the TIR by TSG's TSA algorithm, include (in order of abundance) labradorite, albite and oligoclase. Compositional variations in the albite Na-Ca content are evident and seperate propylitic-associated albite from albite in the inner potassic zone (Figure 2c). Plagioclase

also occurs as a primary feature in all lithologies in the area, being present as crystal fragments in clastic units, and in the groundmass and phenocrysts in coherent units.
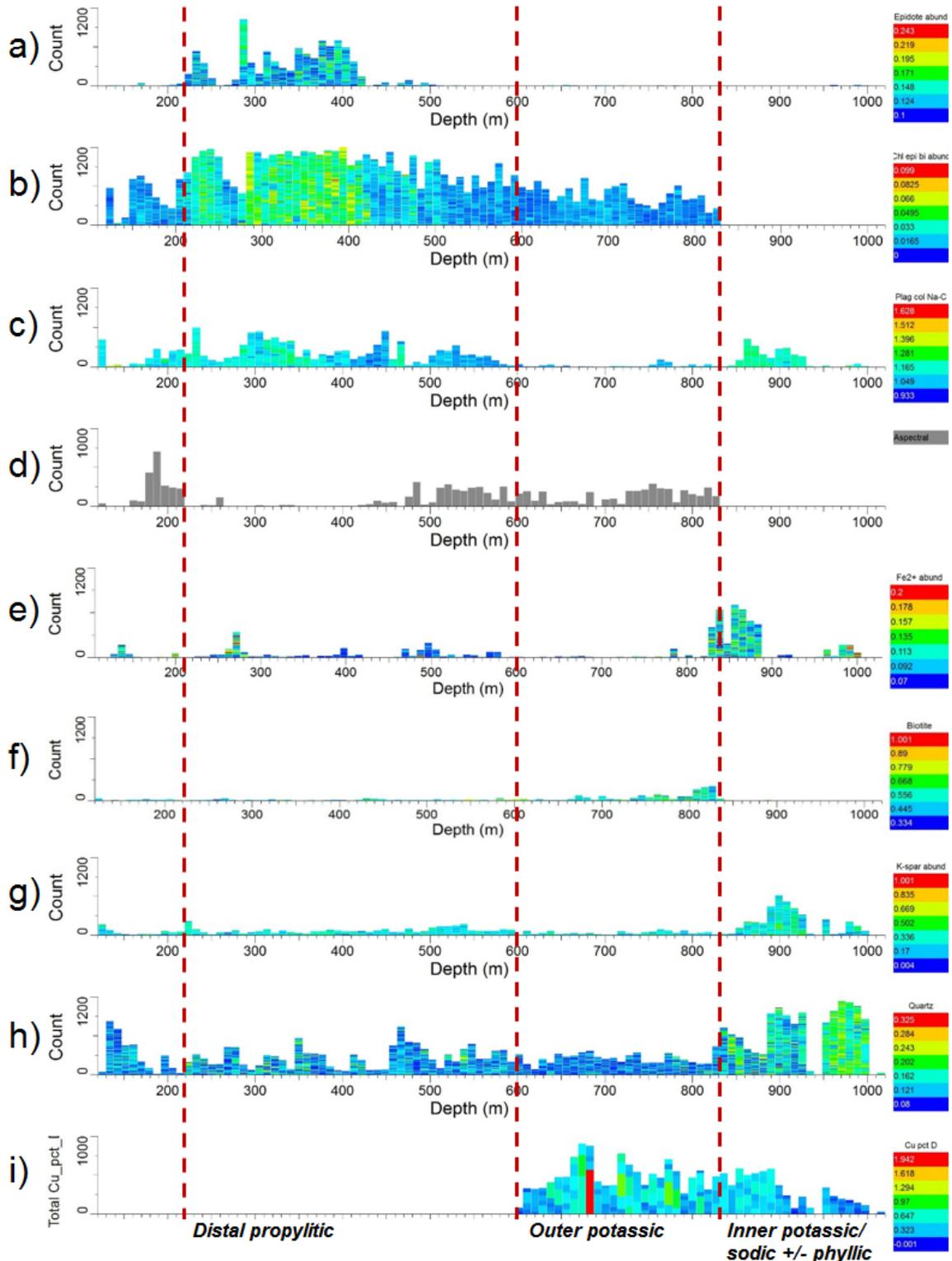
Figure 2.   Downhole spectral responses for key minerals in distal propylitic, and outer potassic alteration zones in hole E48D134 with respect to copper assays. a) epidote abundance. b) combined chlorite-epidote-biotite abundance. c) Albite abundance coloured by Na-Ca composition. d) aspectral response as a proxy for magnetite alteration. e) Fe^{2+} abundance. f) biotite abundance. g) K-feldspar abundance. h) quartz abundance. i) copper assays in wt%.
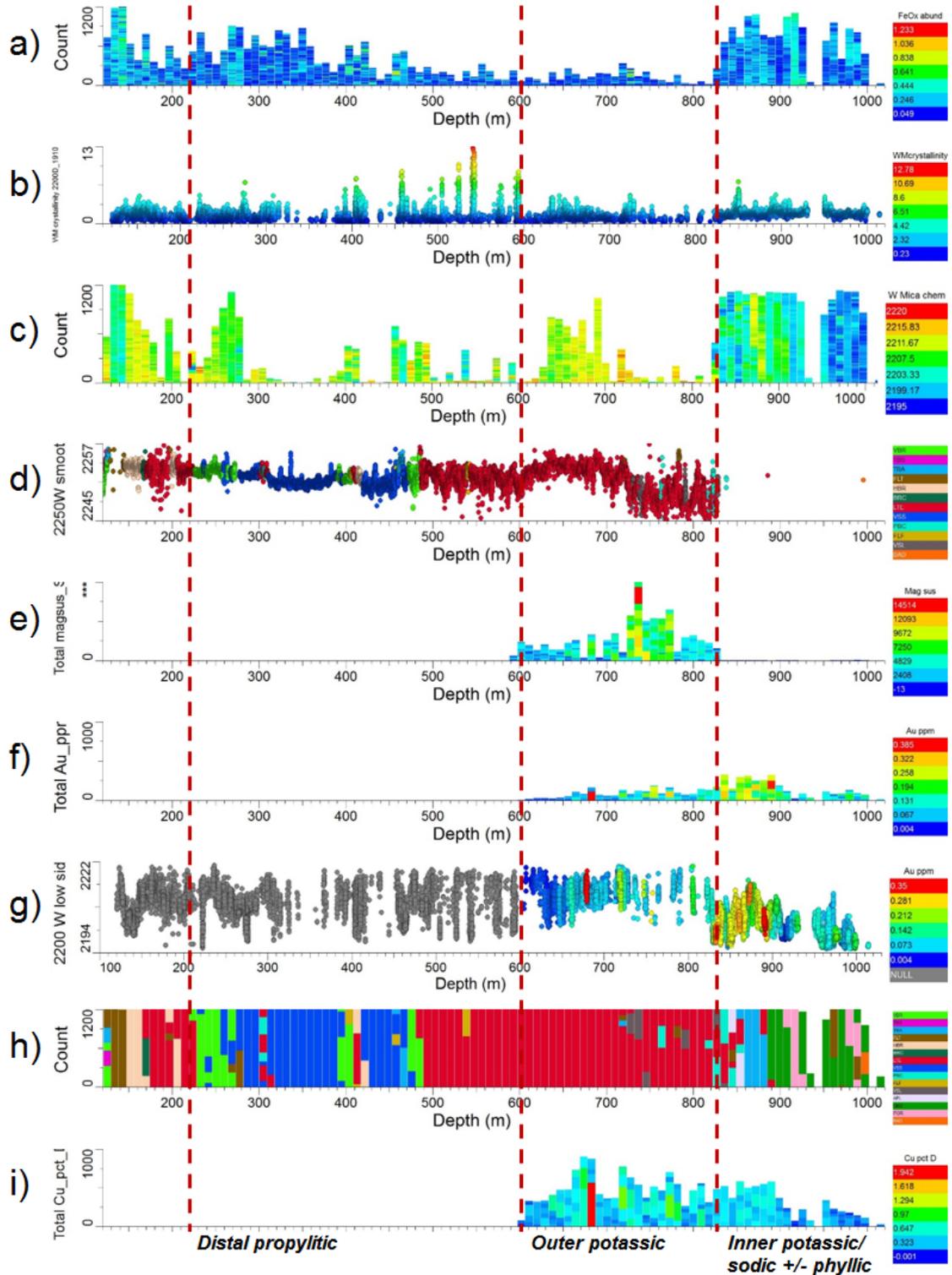
Figure 3.   Downhole spectral responses in inner potassic, and deep phyllic alteration zones in hole E48D134 with respect to copper assays and rock composition. a) FeOx abundance. b) white mica crystallinity. c) white mica abundance coloured by chemistry (wavelength). d) smoothed 2250nm chlorite wavelength coloured by lithology. e) magnetic susceptibility. f) gold assays in ppm. g) 2200nm white mica wavelength coloured by gold assays in ppm. h) host lithology. i) copper assays in wt%.

The detection of multiple plagioclase species may indicate compositional zoning from the core to the rim of the phenocrysts or crystals, or more likely the local replacement of primary sodic-calcic

endmembers by hydrothermal alteration related albite, which commonly occurs as discrete patches associated with epidote in inner propylitic alteration at Northparkes. Petrographic analysis is recommended for confirmation and to further constrain the genetic interpretation.

Narrow intervals of kaolinite and trace dickite characterise the shears associated with the Altona Fault located at the top of the drill hole. Dickite was also identified in the potassic zone by the automated interpretation algorithm in TSG, however an inspection of the spectra determined the TSA result was incorrect. Scalars focussed on the depth and wavelength change of the kaolin/dickite ~2160 – 2180 nm absorption feature produced a more reliable result. This underscores the need to always check the spectra and not treat TSG as a black box.

Outer Potassic Alteration Zone

The outer potassic zone occurs from ~600 m – 830 m and is hyperspectrally characterised by:

- Low abundance biotite/phlogopite.
- Low abundance magnetite (proxy).
- Extensive, moderately abundant chlorite.
- Large gradient change in the chlorite chemistry from Fe-rich to Mg-rich across the Cu-Au ore zone.
- Moderate abundance, extensive plagioclase (labradorite, albite and oligoclase).
- Low abundance, partially extensive muscovite from 630 – 720 m.
- Low abundance carbonate and quartz.
- Trace hornblende.

The outer potassic zone contains the bulk of the Cu ore zone in E48D134 with grades and abundance decreasing down-hole into the inner potassic/sodic zone.

The poorly preserved, low abundance dark mica in the outer potassic zone displays a Fe/Mg-OH related absorption feature at ~2248 nm, indicating a phlogopitic (Mg) composition. The most abundant dark micas occur between ~800-830 m (Figure 2f). The presence of phlogopite (Mg-rich) rather than biotite (Fe-rich) may be explained by the consumption of Fe from the magmatic-hydrothermal fluid to form magnetite and/or chalcopyrite, possibly a function of a higher temperature regime.

Mapping the early biotite-magnetite alteration proved challenging as the biotite/phlogopite is largely retrogressed to chlorite, and magnetite is aspectral (as are most opaque minerals). A proxy for mapping magnetite was derived from the SWIR 'aspectral' result generated by TSG's automated interpretation algorithm, *The Spectral Assistant (TSA)* (Figure 2d). A significant spatial correlation exists between the spectrally logged biotite/phlogopite (Figure 2f) distribution and that of the aspectral result, supporting its use as a magnetite proxy. Aspectral results higher in the hole (180-220m) largely correspond to zones of feldspar-rich lithologies displaying probable patchy albite alteration. This is in line with TIR results, in which most of the aspectral samples display plagioclase (groundmass) spectral features.

The aspectral responses interpreted as a proxy for magnetite alteration extended into the propylitic zone, indicating a gradational (overprinting) contact between the outer margins of the early metasomatic biotite-magnetite alteration and the hydrothermal epidote-chlorite-albite propylitic assemblage.

The high magnetic susceptibility values (Figure 3e) display an inverse spatial relationship with white mica abundance (~630 – 728 m) due to the destruction of magnetite during white mica alteration. The lack of white mica/sericitic alteration in the interval 728 m – 822 m provided a window to partially preserve the earlier biotite-magnetite metasomatic alteration.

Moderately abundant chlorite (Figure 2b) occurs as an alteration product replacing plagioclase, biotite and hornblende. The only interval where remnant hornblende was identified from the infrared spectra is between 427.522 m to 448.568 m and one infrared measurement at 813.572 m.

The spectral parameter tracking the wavelength minima variation in the ~2255 ±10 nm chlorite absorption feature provides a key insight into the most striking characteristic in the outer potassic alteration zone - a distinct gradient change in the wall rock chlorite chemistry reflected in the wavelength shift from a Fe-chlorite (2256 nm @~616 m) to a Mg-chlorite (2245 nm @ 818 m) within the latite and across the high grade part of the Cu-Au ore zone (Figure 4).

The compositional change in the chlorites may be a result of the mildly acidic nature of metal-bearing magmatic-hydrothermal fluids progressively being buffered by wall rock reaction, creating a change in the pH of the environment that would be an effective mechanism for the precipitation of Cu and Au. The heterogeneous nature of the chlorite's Fe/Mg-OH related wavelengths from ~730-830 m may reflect the disequilibrium in the mineral system during sulphide precipitation. The more conformable, homogenous Fe trending chlorite wavelengths between ~620-680 m were likely produced from a cooler, near-neutral fluid that was depleted in Mg.

An alternate hypothesis is that the Fe-Mg chlorite composition change is temperature controlled, with the Mg-chlorite reflective of a more proximal setting to the thermal source, which in this case is interpreted to be the mineralising QMP complexes further downhole.

The visually unrecognisable systematic change in the Fe-Mg content of the chlorite documented in the spectral data has potential for application as a chlorite geothermometer or pH indicator, aiding in vectoring to near-ore environments in an exploration setting.

Trends of increasing Mg content in the chlorite of wall rocks with increasing proximity to mineralisation have been documented in many deposits (Downes et al., 2016; Norman et al., 1991; Wilkinson et al., 2015; Zang and Fyfe, 1995). However, Yang et al. 2005 identified Fe-rich chlorite as occurring preferentially toward the core and the most intensely altered parts of the Tuwu Cu-Au porphyry deposit in China, with Mg-rich chlorite and present on the margin and the relatively weakly altered parts of the hydrothermal alteration system. Each deposit should be assessed independently as mineralogical metrics may vary depending on a number of parameters including; deposit type, host lithology, regional metamorphic grade, composition of the ore fluids, pressure and temperature.

A stark boundary between the outer potassic zone and the inner potassic/sodic zone is evident in the hyperspectral mineral results at 830 m. Most notably the down-hole change from a chlorite dominated domain to a white mica dominated domain.

Inner Potassic/Sodic Alteration Zone

The inner potassic/sodic zone occupies the central position of the deposit and represents the highest temperature alteration within and around the QMP complexes, and pre-mineral monzonite bodies. This zone is host to the majority of the higher grade gold mineralisation and sub-economic to ore-grade copper mineralisation (0.2-0.6% Cu). The inner potassic/sodic zone is hyperspectrally characterised by the presence of:

- Moderately abundant K-feldspar (microcline).
- Abundant quartz.
- Abundant albite.
- Hematitic dusting of feldspars.
- Distinct lack of chlorite.
- Minor ankerite and siderite.
- Abundant white mica (see Deep Phyllic Alteration Zone section below).
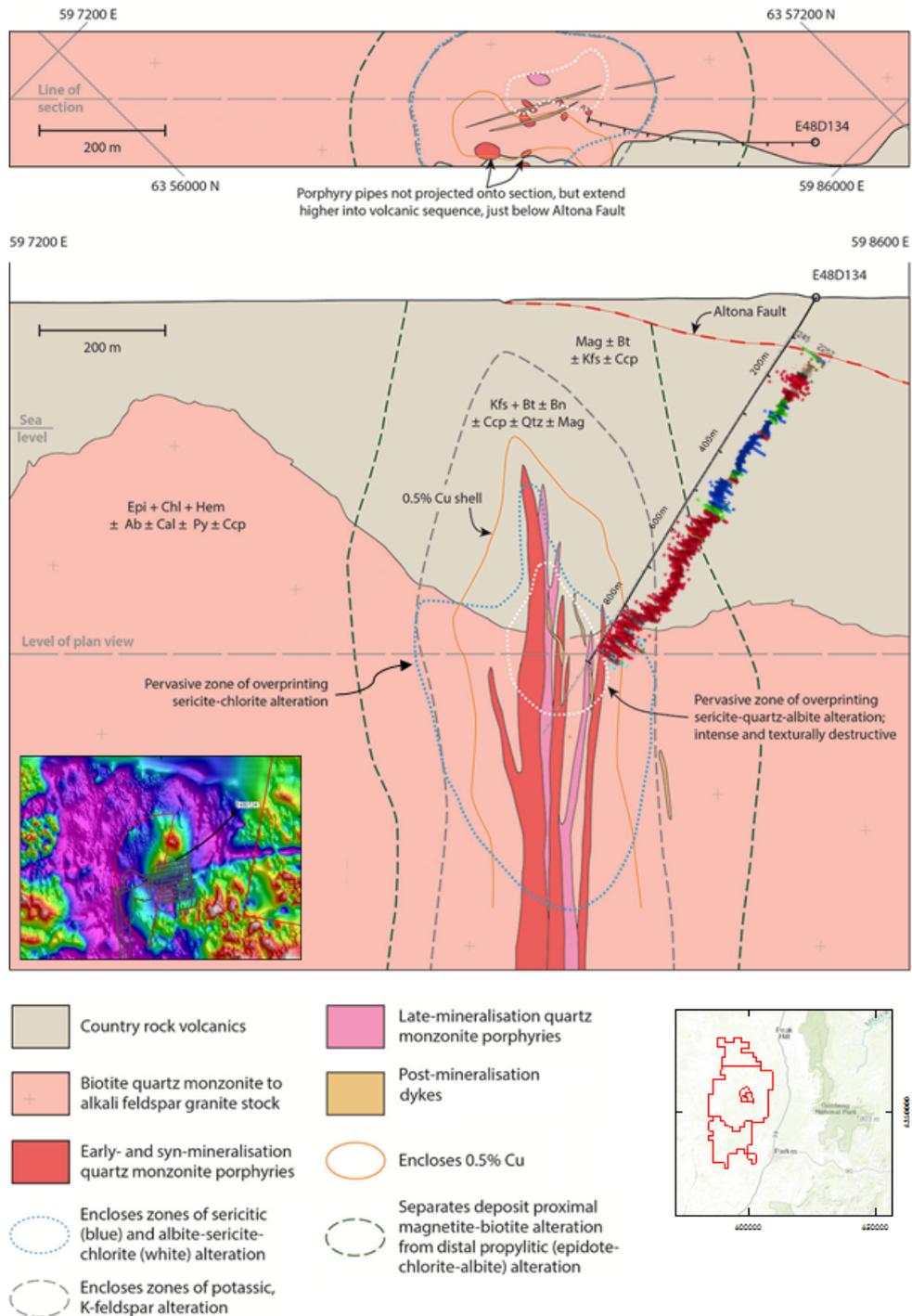
Figure 4.   Schematic oblique northeast-facing section through E48 deposit at Northparkes, with respect to main lithological units, alteration and mineralisation assemblages, and hole for which spectral results are reported (E48D134). Inset map shows hole trace with respect to underground infrastructure and RTP airborne magnetics. Downhole trace adjacent to hole shows smoothed average wavelength shift for 2250nm chlorite absorption feature, showing decreasing wavelength with proximity to porphyry units.

In the high temperature alteration zone, the original rock forming minerals have been replaced by hyperspectrally identified alteration minerals, primarily albite, microcline, quartz and white mica (Figures 2c, 2g, 2h and 3c). The potassic feldspar, microcline, occurs as millimetre-scale selvages/halos to quartz-sulphide veins, as fine aplitic vein dykes emanating off QMP bodies, and replaces plagioclase in the wall rocks.

The plagioclase in this zone differs from the other alteration zones in that it consists of only albite due to Na metasomatism. The albite in the ore zone was spectrally identified as more Na rich compared to the more Ca rich albites in the remainder of the drill hole using an experimental scalar based on (Cudahy et al., 2009) (Figure 2c). This is potentially indicative of a sodic/calc-potassic assemblage, which are developed at deeper levels in a number of alkalic porphyry systems worldwide (Holliday, 2007). This interpretation is supported by the position of E48D134 intercept, at depth on the margins of the high-grade ore shell, where such an assemblage would be expected to occur.

High abundance of spectrally identified quartz and white mica dominate the inner potassic/sodic zone. The white mica constitutes the dominant component of the overprinting phyllic zone discussed in the next section. Quartz was identified by a diagnostic trough in the TIR at ~8625 nm due to stretching lattice vibrations of the Si-O bonds. The high abundance of quartz in the spectra is due to the high density of quartz veining within the core, characteristic of the E48 ore zone where the bulk of the mineralisation is hosted in the magmatic-hydrothermal quartz veins. Multiple stages of quartz veining were observed in the HyLogger imagery. The textural context of the quartz veins could be extracted in an objective systematic approach using a method in development by (Wang et al., 2016) who have undertaken preliminary investigations into an automated approach integrating the HyLogger linescan imagery and spectro-mineralogical results to extract textural information such as quartz vein density.

Widespread hematite dusting of feldspars is noted in hand specimen from this alteration zone, but the dusting was not able to be fully resolved with a scalar targeting the iron oxide crystal field feature at ~900 nm as anticipated. An alternate scalar (Figure 3a) was created to extract samples with a peak at ~750 nm in the visible part of the spectrum, targeting the reddish colour of the rock. The result was successful at selectively discriminating the altered trachyandesite and porphyry units from the quartz monzonites that display a whitish 'bleached' appearance due to intense white mica alteration. The 750 nm scalar represents a hyperspectral metric for identifying the inter-zonal differences in the inner potassic/sodic alteration zone.

Two carbonate composition populations were identified by wavelength changes in the ~6450 nm peak height in the TIR; 1) ankerite occurring in low abundance throughout most of the drill hole and 2) siderite occurring in veins at the peripheries of the inner potassic/sodic alteration zone particularly in the late stage basaltic dykes at the end of the hole.

Deep Phyllic Alteration Zone

The deep phyllic alteration zone is hyperspectrally characterised by the spatial distribution and intensity variations of white mica, ranging in composition from muscovitic to phengitic. This alteration zone overlaps with and crosscuts the inner potassic/sodic alteration zone, with the deep phyllic zone tending to be better developed within the pre- and syn-mineral monzonite intrusives (monzonite and QMPs) compared with the surrounding GVC which tends to host potassic assemblages at depth in E48D134.

Note the gap in the figures from 1000.1 – 1013.9m is due to missing core.

Two generations of phyllic alteration are apparent at depth in E48D134. The most distinct is the pervasive and intense, texturally destructive white mica "bleaching" between ~830-1000 m overprinting earlier potassic and sodic alteration, and is interpreted to represent an event of magmatically derived syn-mineralisation alteration, similar to that described at E26 (Harris and Golding, 2002), where crystallisation may lead to exsolution of magmatic-hydrothermal vapour and fluid within the causative QMPs, altering them and immediately surrounding intrusives and wallrock. The second generation of phyllic alteration is associated with late stage faulting which is characteristic of the other Northparkes deposits.

Three sub-groups of white micas were defined in the ore zone based on the compositional variation spectrally identified by changes in Al substitution in the octahedral site of the white micas (e.g. Tschermak Al substitution in white mica (Al – ⇔[Si+Fe/Mg])). A progressive shift in the AlOH-related wavelengths (e.g. ~2185 – 2225 nm) is indicative of the change in Al content (Duke, 1994). Shorter wavelength muscovitic white micas indicate acidic conditions in the porphyry ore environment and longer wavelength (phengitic) white micas are developed under more neutral conditions (Halley, 2015).

The spatial association between white micas of specific wavelengths and copper-gold mineralisation is indicative of a genetic link between these features, with the deep phyllic alteration developing contemporaneously with copper-gold mineralisation, and anomalous molybdenum values.
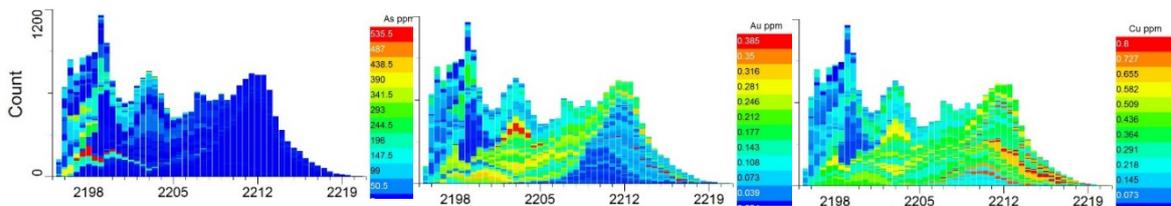
Figure 5.   Three populations of white mica based on Al content (indicated by wavelength minima plotted on X-axis) and their association with As, Au and Cu. A) Short wavelength white mica 2196 – 2200 nm correlated with elevated As (acidic), b) Intermediate wavelength 2201 – 2205 nm correlated with elevated Au (neutral) and c) Long wavelength white mica 2206-2216 nm correlated with elevated Cu (alkaline).

Imported geochemistry assays were integrated with the white mica wavelengths in TSG (Figure 5) and revealed the following correlations with the E48D134 HyLogger data:

- Short wavelength white mica 2196 – 2200 nm correlated with elevated As (acidic).
- Intermediate wavelength 2201 – 2205 nm correlated with elevated Au (acidic-neutral).
- Long wavelength white mica 2206-2216 nm correlated with elevated Cu (neutral).

Based on the correlation, the wavelengths of the white mica alteration indicate the pH conditions within the E48 ore zone ranging from acidic at depth to more neutral as the fluids ascend (Figure 3c). Initially, arsenic was deposited under hot acidic conditions generated from the magmatic-hydrothermal fluids emanating from the causative QMZ intrusions. As the fluids ascended from the intrusions, they cool, becoming more neutral (neutral pH), and gold and copper were deposited.

An unexpected outcome of investigating the phyllic alteration in the ore zone was the detection of anomalous white micas displaying unusual absorption features at 1320 nm and 1840 nm. These features are not typical white mica features and are suspected of indicating fluorine content of the muscovite generated from magmatic-hydrothermal processes/complexes. In these processes, F exchanges for OH in the white mica crystal structure. Fluorine is a smelter penalty element and its hyperspectral detection hosted in white micas may aid the geometallurgical flowsheet planning and processing of ore recovery for E48. Samples will be collected from E48D134 at 848.4 m, 909.09 m and 998.89 m for chemical analysis to verify the interpretation and determine the wt% F.

The frequency of the ankerite and siderite veins increases either side of the intensely developed phyllic zone, marking the boundary between acidic to more neutral fluid conditions at the time of alteration.

CONCLUSIONS

This study documented the mineralogical characteristics of the Northparkes E48 porphyry deposit based on VNIR – SWIR + TIR hyperspectral core logging data captured with a HyLogging system. The dominant minerals identified from the E48D134 HyLogger spectra include plagioclase, quartz and white mica. Subordinate chlorite and epidote are present in moderate abundance. Kaolinite, montmorillonite, goethite, hematite, goethite, gypsum, carbonate, microcline, biotite and phlogopite occur in minor abundance. Trace amounts of dickite and hornblende were also identified.

The distribution and alteration intensity / relative abundance of key minerals identified from the E48D134 HyLogger data enabled the mineralogical logging and spatial delineation of an alteration footprint consisting of four distinct porphyry-related hydrothermal alteration zones and include the following minerals in order of abundance;

> **1) Distal propylitic zone** (~120 – 600 m): Plagioclase, chlorite, epidote, quartz, white mica, hematite/goethite and ankerite.
> **2) Outer potassic zone** (~600 – 830 m): Plagioclase, chlorite, white mica, biotite/phlogopite, magnetite (proxy), ankerite and quartz.
> **3) Inner potassic/sodic zone** (~830 – 1014.15 m): Quartz, white mica (overprinting phyllic), albite, microcline, carbonate.
> **4) Deep phyllic zone overprinting inner potassic/sodic zone** (~830 – 1014.15 m): White mica.

In addition to identifying the mineralogy and characterising the alteration zones, results from this study:

- Reveal previously unknown inter-zonal mineralogical characteristics in the E48 drill core. For example, the visually unrecognisable compositional differences in the chlorite (Fe-Mg) and white micas (Al-Fe/Mg) that provided information on the temperature and pH physicochemical conditions associated with ore formation.
- Demonstrate the integration of hyperspectrally derived mineral results with ancillary exploration datasets (e.g. geochemistry, magnetic susceptibility and lithology).
- Provide a framework to guide future hyperspectral drill core logging at Northparkes using a TerraSpec 4 hand-held spectroradiometer and TSG software.
- Improve the characterisation of the bulk rockmass, potentially reducing the risk in underground development.
- Demonstrate how the spectral fingerprints of minerals can be used to spatially define and characterise the hydrothermal alteration footprints associated with Cu-Au porphyry deposits.

ACKOWLEDGMENT

REFERENCES

Berman, M., Bischof, L., and Hungtington, J., 1999, Algorithms and software for the automated identification of minerals using field spectra or hyperspectral imagery: Thirteenth International Conference on Applied Geologic Remote Sensing, Vancouver., BC., Canada, 1999, p. 222-232.

Berman, M., Bischof, L., Lagerstrom, R., Guo, Y., Huntington, J., Mason, P., and Green, A. A., 2017, A Comparison Between Three Sparse Unmixing Algorithms Using a Large Library of Shortwave Infrared Mineral Spectra: Ieee Transactions on Geoscience and Remote Sensing, v. 55, p. 3588-3610.

Clark, R. N., 1999, Spectroscopy of rocks and minerals and principles of spectroscopy, *in* Rencz, A. N., ed., Remote sensing for the Earth sciences, Manual of remote sensing, 3: New York, John Wiley and Sons, Inc., p. 3-58.

CMOC, 2017, China Molybdenum Co. Ltd Annual Report 2016, p. 240.

Cudahy, T. J., Hewson, R., Caccetta, M., Roache, A., Whitbourn, L., Connor, P., Mason, P., Yang, K., Huntington, J., and Quigley, M., 2009, Drill Core Logging of Plagioclase Feldspar Composition and Other Minerals Associated with Archean Gold Mineralization at Kambalda, Western Australia, Using a Bidirectional Thermal Infrared Reflectance System: Economic Geology, v. 16, p. 223-235.

Downes, P. M., Tilley, D. B., Fitzherbert, J. A., and Clissold, M. E., 2016, Regional metamorphism and the alteration response of selected Silurian to Devonian mineral systems in the Nymagee area, Central Lachlan Orogen, New South Wales: a HyLogger™ case study: Australian Journal of Earth Sciences, v. 63, p. 1027-1052.

Duke, E. F., 1994, Near infrared spectra of muscovite, Tschermak substitution, and metamorphic reaction progress: Implications for remote sensing: Geology, v. 22, p. 621-624.

Glen, R. A., Spencer, R., Willmore, A., David, V., and Scott, R. J., 2007, Junee – Narromine Volcanic Belt, Macquarie Arc, Lachlan Orogen, New South Wales: components and structure: Australian Journal of Earth Sciences, v. 54, p. 215-241.

Glen, R. A., Walshe, J. L., Barron, L. M., and Watkins, J. J., 1998, Ordovician convergent-margin volcanism and tectonism in the Lachlan sector of east Gondwana: Geology, v. 26, p. 751-754.

Halley, S., Dilles, J. H., & Tosdal, R. M., 2015, Footprints: Hydrothermal alteration and geochemical dispersion around porphyry copper deposits, 100Society of Economic Geologists Newsletter, p. 1-17.

Harris, A. C., and Golding, S. D., 2002, New evidence of magmatic-fluid–related phyllic alteration: Implications for the genesis of porphyry Cu deposits: Geology, v. 30, p. 335-338.

Holliday, J. R. a. C., D. R, 2007, Advances in geological models and exploration methods for copper ± gold porphyry deposits: Exploration 07: Fifth Decennial International Conference on Mineral Exploration, Toronto, Canada, September 9-12, 2007, p. 791-809.

House, M. J., 1994, Gold distribution at the E26 porphyry copper-gold deposit, Goonumbla N.S.W.: Unpub. MSc thesis, University of Tasmania, 125 p.

Hunt, G. R., 1977, Spectral signatures of particulate minerals in the visible and near infrared: Geophysics, v. 42, p. 501-513.

Hunt, G. R., and Salisbury, J. W., 1970, Visible and near-infrared spectra of minerals and rocks - (pt.) 1, silicate minerals: Modern Geology, v. 1, p. 283-300.

Huntington, J., Quigley, M., Yang, K., Roache, T., Young, C., Roberts, I., Whitbourn, L., and Mason, P., 2006, A geological overview of HyLogging 18 000 m of core from the Eastern Goldfields of Western Australia, *in* Dominy, S., ed., 6th International Mining Geology Conference.

Australasian Institute of Mining and Metallurgy Publication Series: Parkville Victoria, Australasian Inst Mining & Metallurgy, p. 45-50.

Huntington J. F., W. L. B., Quigley M. A., Yang K., Mason, and P., C. T. J., Connor P., Coward D., Hewson R. & Phillips R., 2008. Development and implementation of advanced automated core logging technology for enhanced mine feasibility and development in Western Australia, Minerals and Energy Research Institute of Western Australia. Report 269. p.

Lickfold, V., Cooke, D. R., Crawford, A. J., and Fanning, C. M., 2007, Shoshonitic magmatism and the formation of the Northparkes porphyry Cu – Au deposits, New South Wales: Australian Journal of Earth Sciences, v. 54, p. 417-444.

Lickfold, V., Cooke, D. R., Smith, S. G., and Ullrich, T. D., 2003, Endeavour Copper-Gold Porphyry Deposits, Northparkes, New South Wales: Intrusive History and Fluid Evolution: Economic Geology, v. 98, p. 1607-1636.

Lye, A., 2010, Forty years on and still prospective - the Northparkes story, in Lewis, P. C., ed., Mines & Wines 2010: Mineral Exploration in the Tasmanides: Mudgee, AustraliaAustralian Institute of Geoscientists, p. 93-99.

Lye, A., Crook, G. and Kolff van Oosterwijk, L., 2006, The Discovery History of the Northparkes Deposits: Mines & Wines Conference, Cessnock NSW, 25-26 May 2006, 2006, p. 5.

Norman, D. K., Parry, W. T., and Bowman, J. R., 1991, Petrology and geochemistry of propylitic alteration at Southwest Tintic, Utah: Economic Geology, v. 86, p. 13-28.

Quigley, M. A., Huntington, J.F., Whitbourn, L.W., Munday, T., Yang, K., Schodlok, M.C, 2009, HyLogging: core logging technologies heading to operational uptake, Geological Remote Sensing Group AGM "Exploration Remote Sensing", P2010/129: London, U.K.

Schodlok, M. C., Whitbourn, L., Huntington, J., Mason, P., Green, A., Berman, M., Coward, D., Connor, P., Wright, W., Jolivet, M., and Martinez, R., 2016, HyLogger-3, a visible to shortwave and thermal infrared reflectance spectrometer system for drill core logging: functional description: Australian Journal of Earth Sciences, v. 63, p. 929-940.

Simpson, C., Cas, R.A.F., and Arundell, M.C., 2000., 2000, The Goonumbla Caldera, Parkes, NSW: fact or fiction?: Abstracts for the 15th Australian Geological Convention. Understanding planet earth: Searching for a sustainable future, Sydney, Australia, 2000, p. 452.

Wang, D., Lagerstrom, R., Sun, C., Laukamp, C., Quigley, M., Whitbourn, L., Mason, P., Connor, P., and Fisher, L., 2016, Automated vein detection for drill core analysis by fusion of hyperspectral and visible image data: 2016 23rd International Conference on Mechatronics and Machine Vision in Practice (M2VIP), Nanjing, China, 28-30 Nov. 2016, 2016, p. 1-6.

Wilkinson, J. J., Chang, Z., Cooke, D. R., Baker, M. J., Wilkinson, C. C., Inglis, S., Chen, H., and Bruce Gemmell, J., 2015, The chlorite proximitor: A new tool for detecting porphyry ore deposits: Journal of Geochemical Exploration, v. 152, p. 10-26.

Wolfe, R. C., 1994, The geology, paragenesis and alteration geochemistry of the Endeavour 48 Cu-Au porphyry, Goonumbla N.S.W.: Unpub. BSc (Hons) thesis, University of Tasmania, 102 p.

Zang, W., and Fyfe, W. S., 1995, Chloritization of the hydrothermally altered bedrock at the Igarapé Bahia gold deposit, Carajás, Brazil: Mineralium Deposita, v. 30, p. 30-38.